Optimizing the FEDVR-TDCC code for exploring the quantum dynamics of two-electron systems in intense laser pulses

S. X. Hu*

Laboratory for Laser Energetics, University of Rochester, 250 E. River Road, Rochester, New York 14623, USA

(Received 12 February 2010; published 19 May 2010)

To efficiently solve the three-dimensional (3D) time-dependent linear and nonlinear Schrödinger equation, we have developed a large-scale parallel code RSP-FEDVR [B. I. Schneider, L. A. Collins, and S. X. Hu, Phys. Rev. E **73**, 036708 (2006)], which combines the finite-element discrete variable representation (FEDVR) with the real-space product algorithm. Using the similar algorithm, we have derived an accurate approach to solve the time-dependent close-coupling (TDCC) equation for exploring two-electron dynamics in linearly polarized intense laser pulses. However, when the number (N) of partial waves used for the TDCC expansion increases, the FEDVR-TDCC code unfortunately slows down, because the potential-matrix operation scales as $\sim O(N^2)$. In this paper, we show that the full potential-matrix operation can be decomposed into a series of small-matrix operations utilizing the sparse property of the $[N\times N]$ potential matrix. Such optimization speeds up the FEDVR-TDCC code by an order of magnitude for $N=256$. This may facilitate the ultimate solution to the 3D two-electron quantum dynamics in ultrashort intense optical laser pulses, where a large number of partial waves are required.

DOI: 10.1103/PhysRevE.81.056705 PACS number(s): 02.70.Dh, 32.80.Rm

I. INTRODUCTION

Electron correlation plays an essential role in understanding many-body phenomena ranging from atomic structure formation, superconductivity, to chemical reactions. Even for few-body atomic systems such as Helium, it has been a challenge to fully explore electron-electron interactions, especially in the case that the system is under strong driving by external forces. For example, in the single-photon induced double-ionization process of He, it is difficult to have an insight into the dynamical energy sharing between the two electrons without full quantum-mechanics calculations [1]. Another example is the appearance of the "kneelike" double ionization signal of He exposed to intense optical laser pulses [2–7], where electron-electron interaction is the key to understand the nonsequential multiple ionizations in intense laser-driven multielectron atoms [8]. Progress has been made recently for both time-dependent and time-independent calculations of single- and double-photon double ionization of He, which have taken the full electron correlation into account [9–17]. However, when more and more photons involved in the two-electron ionization process, it has become very difficult for full-dimensional quantum calculations of He exposed to intense optical laser pulses, although there have been attempts to attack such a hard problem by directly discretizing the five-dimensional spatial grid in past years [18,19].

For a two-electron system exposed to intense laser pulses, a large and fine-enough spatial grid is demanded to well accommodate and characterize the fast moving electron wave packets. Equal-spacing grid requires enormous number of points to span the space, which is unaffordable even with nowadays supercomputers. While, variable-size grid [20] cannot be easily implemented with finite-difference (FD) based algorithms. To flexibly place fine grids to where they are needed, we have found that the finite-element discrete variable representation (FEDVR) has great advantages over the FD-based method [21–24]. In the FEDVR method, one naturally divides the space into various-size finite elements along each dimension. In the Cartesian coordinate, these finite elements along x, y, and z axis are orthogonal and can be directly taken their product to represent the three-dimensional (3D) space. Within each finite element, one can in principle use any complete basis function, such as the Legendre polynomial [24] or the Fourier function [25], to represent the wave function in arbitrary order, though the connection between neighbor elements needs special care. Under such a representation, the kinetic-energy operator are *block diagonal* and each block acts separately on the wave function within its corresponding finite element. The sparse kinetic-energy matrix can therefore be decomposed into *even* and *odd* blocks, which alternatively act on the wave function in the fashion of the real-space product (RSP) algorithm [26]. For two-electron system, using the time-dependent close-coupling (TDCC) method [27] one can expand the two-electron wave function in terms of bipolar spherical harmonics (partial waves). Thus, the resulting potential-energy matrix couples the N partial waves used in the expansion. In the previous implementation of the FEDVR-TDCC code [24], we have directly diagonalized the potential-energy matrix and made its action on the wave function by $N\times N$ matrix operations, which obviously scales as $\sim O(N^2)$. Calculations using such implemented FEDVR-TDCC code have been performed for x-ray interactions with He [28–30], for electron-Rydberg-atom collisions [31], and for three-body electron-ion recombinations [32], in which less than 100 partial waves were involved in the expansion. However, when the total partial waves (N) increases, as is in the case of He exposed to intense optical pulses, the full-matrix operation got so slow that such *ab initio* studies become impractical. Full-dimensional quantum calculations for two-electron sys-

*shu@lle.rochester.edu

 ©2010 The American Physical Society

tems driven by intense optical laser pulses has long been sought for advancing our understanding of electron correlations in the strong-field physics community. The technique demonstrated in this paper shall make such complete calculations practical.

We will show that the full $(N\times N)$ potential-energy matrix has special features which can be utilized for speeding up the FEDVR-TDCC code. For example, the electron-nucleus Coulomb interaction matrix is diagonal, while the electron-electron interaction matrix is block diagonal in which only those partial waves having same total angular-momentum quantum number coupling to each other. Moreover, for linearly polarized laser pulses the laser-electron interaction matrix is *block tridiagonal*. Thus, the $N\times N$ potential-energy matrix is still sparse so that we can utilize this property to further optimize the FEDVR-TDCC code, by decomposing them into a series of small-matrix operations. In Sec. II, we shall layout the fundamentals of using the time-dependent close-coupling method to solve the two-electron Schrödinger equation under the FEDVR scheme. We then describe how to enhance the code performance by further decomposing the $N\times N$ potential-energy matrix operations into a series of small-matrix operations in Sec. III. Numerical testing results and discussions will be presented in Sec. IV. Finally, we shall summarize the paper.

II. RSP-FEDVR-TDCC METHOD FOR TWO-ELECTRON DYNAMICS IN INTENSE LASER PULSES

To investigate the dynamics of two-electron quantum systems (in a central potential with nuclear charge Z) exposed to intense laser pulses, we solve the following time-dependent Schrödinger equation in full dimensions (atomic units are used throughout),

$$i\frac{\partial\Phi(\mathbf{r}_1,\mathbf{r}_2;t)}{\partial t} = \left[\Delta_{\mathbf{r}_1} + \Delta_{\mathbf{r}_2} - \frac{Z}{r_1} - \frac{Z}{r_2} + \frac{1}{|\mathbf{r}_1-\mathbf{r}_2|} + \mathbf{E}(t)\cdot(\mathbf{r}_1+\mathbf{r}_2)\right]\Phi(\mathbf{r}_1,\mathbf{r}_2|t), \tag{1}$$

where Δ is the Laplace operator in three dimensions, and variables with bold face represent vectors. Namely, $\mathbf{r}_1$ and $\mathbf{r}_2$ are the position vectors of the two electrons with respect to the nucleus at the origin. The usual dipole approximation is used for the laser-electron coupling. It is computationally intractable to numerically solve Eq. (1) in its full six dimensions. Instead, we can use the time-dependent close-coupling method [27] to obtain a tractable form of Eq. (1). Namely, for the motion of two electrons in a central potential, we can expand the total wave function $\Phi(\mathbf{r}_1,\mathbf{r}_2;t)$ in terms of the bipolar spherical harmonics, $\mathcal{Y}^{L,M}_{l_1l_2}(\Omega_1,\Omega_2) = \Sigma_{m_1m_2} C^{LM}_{l_1m_1l_2m_2} Y_{l_1m_1}(\theta_1,\phi_1) Y_{l_2m_2}(\theta_2,\phi_2)$ with the Clebsch-Gordan coefficients $C^{LM}_{l_1m_1l_2m_2}$ for the symmetry (LM),

$$\Phi(\mathbf{r}_1,\mathbf{r}_2;t) = \sum_{LM}\sum_{l_1l_2}\frac{\Psi^{(LM)}_{l_1l_2}(r_1,r_2;t)}{r_1r_2}\mathcal{Y}^{L,M}_{l_1l_2}(\Omega_1,\Omega_2). \tag{2}$$

We note that the electron-electron Coulomb repulsion term $1/|\mathbf{r}_1-\mathbf{r}_2|$ and the field interaction terms $\mathbf{E}(t)\cdot(\mathbf{r}_1+\mathbf{r}_2)$ can also be expanded in terms of bipolar spherical harmonics:

$$\frac{1}{|\mathbf{r}_1-\mathbf{r}_2|} = \sum_{l=0}^{\infty}\frac{(-1)^l 4\pi}{\sqrt{2l+1}}\times\frac{r_<^l}{r_>^{l+1}}\mathcal{Y}^{0,0}_{ll}(\Omega_1,\Omega_2) \tag{3}$$

where $r_<=\min(r_1,r_2)$ and $r_>=\max(r_1,r_2)$ and for linearly polarized pulse (say, polarization along z axis),

$$\mathbf{E}(t)\cdot(\mathbf{r}_1+\mathbf{r}_2) = \frac{4\pi}{\sqrt{3}}E(t)[r_1\mathcal{Y}^{1,0}_{10}(\Omega_1,\Omega_2) + r_2\mathcal{Y}^{1,0}_{01}(\Omega_1,\Omega_2)]. \tag{4}$$

From now on, we drop the M dependence in the expansions for the case of linear polarization $(M=0)$.

Substituting these expansions into the above Schrödinger equation (1) and integrating over the angles Ω_1 and Ω_2 (taking into account the orthonormal properties of spherical harmonics) yields a set of coupled partial differential equations,

$$\begin{aligned} i\frac{\partial}{\partial t}\Psi^L_{l_1l_2}(r_1,r_2;t) &= [\hat{T}+\hat{V}_c]\Psi^L_{l_1l_2}(r_1,r_2;t) \\ &+ \sum_{L'}\sum_{l_1'l_2'}\sum_{l=0}^{\infty}\frac{4\pi(-1)^l}{\sqrt{2l+1}}\frac{r_<^l}{r_>^{l+1}}F_0\Psi^{L'}_{l_1'l_2'}(r_1,r_2;t) \\ &+ \sum_{L'}\sum_{l_1'l_2'}\frac{4\pi}{\sqrt{3}}E(t)[r_1F_1 \\ &+ r_2F_2]\Psi^{L'}_{l_1'l_2'}(r_1,r_2;t), \end{aligned} \tag{5}$$

where the kinetic-energy operator $\hat{T}=\hat{T}_1+\hat{T}_2$ and the potential-energy operator $\hat{V}_c$ for the coupling between nucleus and electrons can be expressed as

$$\hat{T} = \hat{T}_1+\hat{T}_2 = -\frac{1}{2}\frac{\partial^2}{\partial r_1^2} - \frac{1}{2}\frac{\partial^2}{\partial r_2^2}, \tag{6}$$

$$V_c(r_1,r_2) = \frac{l_1(l_1+1)}{2r_1^2} + \frac{l_2(l_2+1)}{2r_2^2} - \frac{Z}{r_1} - \frac{Z}{r_2}. \tag{7}$$

While, the second and third terms in the right hand of Eq. (5) represent the electron-electron Coulomb repulsion and the laser-electron coupling, respectively. The angular-momentum dependent coupling functions have the following forms:

$$F_0 = \sqrt{(2l+1)^2(2l_1'+1)(2l_2'+1)(2L'+1)}/(4\pi)^2 \times C^{l_10}_{l0l_1'0}C^{l_20}_{l0l_2'0}C^{L0}_{00L'0}\times\begin{Bmatrix} l & l_1' & l_1 \\ l & l_2' & l_2 \\ 0 & L' & L\end{Bmatrix}, \tag{8}$$

$$F_1 = \sqrt{9(2l_1'+1)(2l_2'+1)(2L'+1)}/(4\pi)^2 \times C^{l_10}_{10l_1'0}C^{l_20}_{00l_2'0}C^{L0}_{10L'0}\times\begin{Bmatrix} 1 & l_1' & l_1 \\ 0 & l_2' & l_2 \\ 1 & L' & L\end{Bmatrix}, \tag{9}$$

$$F_2 = \sqrt{9(2l_1'+1)(2l_2'+1)(2L'+1)}/(4\pi)^2 \times C^{l_1 0}_{00l_1'0} C^{l_2 0}_{10l_2'0} C^{L0}_{10L'0} \times \begin{Bmatrix} 0 & l_1' & l_1 \\ 1 & l_2' & l_2 \\ 1 & L' & L \end{Bmatrix}, \quad (10)$$

in which the Clebsch-Gordan coefficients (C) and the $9j$ symbols are involved. By using the partial-wave indexing, the coupled Eq. (5) can be rewritten in the following compact form:

$$i\frac{\partial}{\partial t}\Psi_i(r_1,r_2;t) = [\hat{T}+\hat{V}_c]\Psi_i(r_1,r_2;t) + \sum_j [\hat{V}_{F0}(i,j)+\hat{V}_{F12}(i,j)]\Psi_j(r_1,r_2;t), \quad (11)$$

where the partial-wave index i or j stands for a combination of angular-momentum numbers $(l_1 l_2 L)$ or $(l_1' l_2' L')$. The nondiagonal potential matrix $\hat{V}_{F0}$ and $\hat{V}_{F12}$ can be expressed in terms of the above functions of F_0, F_1, and F_2,

$$\hat{V}_{F0}(i,j) = \sum_{l=0}^{\infty} \frac{4\pi(-1)^l}{\sqrt{2l+1}} \frac{r_<^l}{r_>^{l+1}} F_0(i,j), \quad (12)$$

$$\hat{V}_{F12}(i,j) = \frac{4\pi}{\sqrt{3}} E(t)[r_1 F_1(i,j) + r_2 F_2(i,j)]. \quad (13)$$

To discretize the radial space r_1 and r_2, we have used the FEDVR, which has great advantages over the FD-based method [21–24]. In the FEDVR method, one naturally divide r_1 and r_2 into various-size finite elements. Within each finite element, we use the Legendre polynomial [24] as the basis DVR function to represent the wave function in arbitrary order (M). The connection between neighbor elements can be done by using a bridge function that guarantees the continuity across the element boundaries. The potential-energy matrix as well as the kinetic-energy matrix can be easily evaluated by the M-point quadrature rule. Details about the FEDVR method have been presented in Ref. [24].

There are many numerical implementations for solving the coupled partial differential Eq. (11), such as the "staggered leapfrog." However, in order to keep the unitary propagation of the Schrödinger equation, these methods can require very small time-steps. It can become very time-consuming, particularly for calculations where large radial meshes and many partial waves are required. For these considerations, we have applied the RSP [26] algorithm to propagate the coupled wave functions. The RSP algorithm automatically guarantees a unitary propagation and significantly reduces the computational efforts. Implementing with three-point finite difference, the original idea of RSP [26] was to split the tridiagonal kinetic-energy matrix into a series of even and odd 2×2 matrices, which alternatively acts on the corresponding wave function. The similar idea was also working for splitting the total Hamiltonian into the kinetic-energy part and the potential part. By gathering the total N partial waves [at a radial point (r_1,r_2)] into a column vector, i.e.,

$$[\Psi_i(r_1,r_2;t)] = \begin{bmatrix} \Psi_1(r_1,r_2;t) \\ \Psi_2(r_1,r_2;t) \\ \vdots \\ \Psi_i(r_1,r_2;t) \\ \vdots \\ \Psi_N(r_1,r_2;t) \end{bmatrix}, \quad (14)$$

one can approximate the temporal propagation of the coupled wave functions from time t to $t+\Delta t$ to have the following form [with an accuracy of $\sim(\Delta t)^3$]:

$$[\Psi_i(r_1,r_2;t+\Delta t)] = \exp\left[-\frac{i\Delta t}{2}T\hat{I}\right]\exp\left[-\frac{i\Delta t}{2}V_c\hat{I}\right] \times \exp\{-i\Delta t[\hat{V}_F]_{ij}\} \times \exp\left[-\frac{i\Delta t}{2}V_c\hat{I}\right]\exp\left[-\frac{i\Delta t}{2}T\hat{I}\right] \times [\Psi_i(r_1,r_2;t)], \quad (15)$$

where $\hat{I}$ is the $N\times N$ unitary matrix, and the nondiagonal potential-energy operator $[\hat{V}_F]_{ij}=\hat{V}_{F0}(i,j)+\hat{V}_{F12}(i,j)$, which is "sandwiched" by the kinetic energy and the diagonal potential-energy operators. The diagonal action of the exponential potential V_c just contributes a phase shift to each partial wave. The only part that requires specific treatment is the nondiagonal potential operator $[\hat{V}_F]_{ij}$, which is a $N\times N$ matrix that couples the partial waves at each radial point (r_1,r_2). Therefore, for its exponential operation on the partial waves, we must diagonalize this matrix first, i.e., $[D^{-1}][\hat{V}_F]_{ij}[D]=\hat{I}\lambda$, followed by the operation

$$e^{-i\Delta t[\hat{V}_F]_{ij}}[\Psi_i] = [D]e^{-i\Delta t\lambda\hat{I}}[D^{-1}][\Psi_i], \quad (16)$$

at each radial point (r_1,r_2). The diagonalization matrix $[D]$ and its inverse matrix $[D^{-1}]$ are also N by N matrices. One needs to diagonalize the matrix $[\hat{V}_F]_{ij}$ only once for each grid point (r_1,r_2) before the temporal propagation starts. The stored matrices $[D]$, $[D^{-1}]$, and the column vector λ (consisting of eigenvalues of $[\hat{V}_F]_{ij}$) can be used throughout the temporal propagation [24]. It is noted that the field term $E(t)$ can directly multiple the eigenvalue vector λ in the exponential factor. Obviously, such an implementation requires $N\times N$ matrix operation for each spatial point (r_1,r_2), which can significantly slow down calculations as the number of partial waves N becomes large.

III. OPTIMIZING THE NON-DIAGONAL POTENTIAL-ENERGY MATRIX OPERATION

As we discussed above, the nondiagonal potential-energy operator $[\hat{V}_F]_{ij}$ consists of the electron-electron Coulomb repulsion $\hat{V}_{F0}(i,j)$ and the laser-electron coupling $\hat{V}_{F12}(i,j)$.

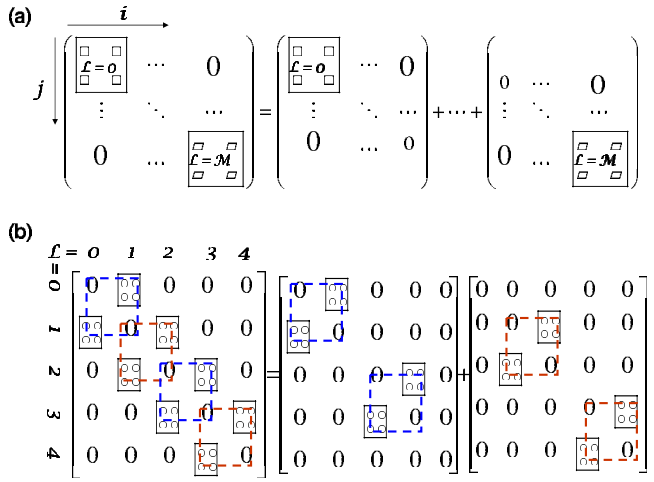

FIG. 1. (Color online) The schematics for decomposing (a) the block-diagonal electron-electron coupling matrix $[\hat{V}_{F0}(i,j)]$ and (b) the linearly polarized laser-electron coupling matrix $[\hat{V}_{F12}]_{ij}$, which is block tridiagonal.

Each of them is a $N\times N$ matrix. The full diagonalization of $[\hat{V}_F]_{ij}$ and carrying out the operation such as Eq. (16) are very expansive when the number of partial waves N becomes large, as it scales as $\sim O(N^2)$. Taking a close look at the matrix structures of $\hat{V}_{F0}(i,j)$ and $[\hat{V}_{F12}]_{ij}$, we find that the former is block diagonal and the latter is block tridiagonal (for linearly polarized fields). This is due to the following properties of the Clebsch-Gordan coefficients:

$$C^{L0}_{00L'0} = 0 \quad \text{for} \quad L' \neq L,$$

$$C^{L0}_{00L'0} = 1 \quad \text{for} \quad L' = L, \tag{17}$$

and

$$C^{L0}_{10L'0} = 0 \quad \text{if} \quad |L' - L| \neq 1, \tag{18}$$

in Eqs. (8)–(10). Namely, the matrices $[\hat{V}_{F0}(i,j)]$ and $[\hat{V}_{F12}]_{ij}$ are still sparse and can be further optimized for fast operations.

To be specific, if we organize the same total angular-momentum partial waves in adjacent indices, the electron-electron interaction matrix $[\hat{V}_{F0}(i,j)]$ is block diagonal since the partial waves couple to each other only within the same total angular momentum. Therefore, it can be decomposed into a sum of relatively small nonzero block matrices, each of that corresponds to a specific total angular momentum L. This is schematically shown by Fig. 1(a), where each "square" represents a nonzero block matrix having the same total angular momentum. For the case of the maximum total angular momentum $L=M$ (L starting from 0), we can decompose the $N\times N$ matrix into $M+1$ nonoverlapping small $n_L \times n_L$ matrices ($[\hat{V}_{F0B}]_L$). Here, n_L is the number of partial waves having the same total angular momentum L. We then have the relationship of $N=\sum_{L=0}^{L=M} n_L$ and n_L can be much smaller than the total number of partial waves N. Thus, instead of doing the $N\times N$ operation, we now need only perform the fast $n_L\times n_L$ matrix multiplication by $M+1$ times, that is,

$$e^{-i\Delta t[\hat{V}_{F0}]} = \Pi_{L=0}^{M} e^{-i\Delta t[\hat{V}_{F0B}]_L}. \tag{19}$$

Namely, each $n_L\times n_L$ exponential matrix operation acts on the corresponding subspace of the total partial waves.

The similar idea can also work for the laser-electron coupling matrix. As is indicated in Fig. 1(b), the matrix $[\hat{V}_{F12}]_{ij}$ is block tridiagonal since for linearly polarized laser pulses the partial-wave coupling only occurs between those that have adjacent total angular momentum L. For example, the $L=1$ partial waves only couple to the $L=0$ and $L=2$ partial waves. In Fig. 1(b), each "0" in the diagram represents a zero block matrix. Each nonzero block belongs to a coupling matrix between the partial waves having adjacent total angular momentum. For instance, the second block in the first row represents the coupling matrix elements between the $L=0$ and $L=1$ partial waves. Thus, we can further decompose such a sparse and block-tridiagonal matrix into the sum of relatively small and nonoverlapping even ($[\hat{V}_{F12}]_{\text{even}}$) and odd ($[\hat{V}_{F12}]_{\text{odd}}$) 2×2-block matrices. Each of them can alternatively act on the corresponding partial waves. To wrap it up, we write the procedure in the following form:

$$\begin{aligned}\exp(-i\Delta t[\hat{V}_{F12}]) = {} & \exp\left(-i\frac{\Delta t}{2}[\hat{V}_{F12}]_{\text{odd}}\right) \\ & \times \exp(-i\Delta t[\hat{V}_{F12}]_{\text{even}}) \\ & \times \exp\left(-i\frac{\Delta t}{2}[\hat{V}_{F12}]_{\text{odd}}\right).\end{aligned} \tag{20}$$

Splitting the block-tridiagonal matrix into even and odd small 2×2 block matrices is similar to the idea of splitting the kinetic and potential matrices in Eq. (15), which results in the similar accuracy to the order $\sim(\Delta t)^3$. Again, each of these 2×2-block matrices are smaller than the total $N\times N$ matrix, so that such decomposition can be very helpful for large N.

Finally, we summarize the above optimization procedures in the following "sandwich" form, for the nondiagonal potential-energy propagator in Eq. (15),

$$\begin{aligned}\exp\{-i\Delta t[\hat{V}_F]\} = {} & \Pi_{L=0}^{M} \exp\left\{-i\frac{\Delta t}{2}[\hat{V}_{F0B}]_L\right\} \\ & \times \exp\left\{-i\frac{\Delta t}{2}[\hat{V}_{F12}]_{\text{odd}}\right\} \\ & \times \exp\{-i\Delta t[\hat{V}_{F12}]_{\text{even}}\} \\ & \times \exp\left\{-i\frac{\Delta t}{2}[\hat{V}_{F12}]_{\text{odd}}\right\} \\ & \times \Pi_{L=0}^{M} \exp\left\{-i\frac{\Delta t}{2}[\hat{V}_{F0B}]_L\right\}.\end{aligned} \tag{21}$$

Such optimizations can significantly reduce the time cost for the potential propagator. It is noted that the two-dimensional domain decomposition has been used to parallelize the radial

spaces with the message-passing interface (MPI) scheme [24].

IV. RESULTS AND DISCUSSIONS

We have explored the quantum dynamics of He exposed to an intense few-cycle pulse (FCP). In the radial space r_1 and r_2, we have used 160 finite elements with FE-sizes varying from 0.4 to 1.2 bohr. A five-point DVR has been applied within each finite element. The grid of 641 DVR points in each dimension spans a radial space up to ~175.8 a.u., with the smallest $\Delta r \simeq 0.069$ bohr. Using this grid, we have dumped a wave packet in imaginary time to get the ground state of He. Eight partial waves ($l_1=l_2=0-7$ and $L=0$) have been included in the imaginary-time propagation for ~0.5 fs with a time step $\Delta t \simeq 4.1\times 10^{-3}$ a.u.. Finally, we obtained a very accurate ground state of He with energy of $E_0 \simeq -2.9015$ a.u., which is well compared with the theoretical and experimental value of $E_0 \simeq -2.9033$ a.u.. It is also noted that the TDCC method has been extensively used for calculations of single- or two-photon double ionization of He by XUV pulses. Those calculations have been well compared with experimental results and benchmarked with other methods in Refs. [33,34]. This paper is devoted to show how we can speed up such full-dimensional quantum calculations.

Using the same grid setup, we have studied how the ground-state He responds to an intense few-cycle optical pulse. The FCP is shown in Fig. 2(a), which has a wavelength of $\lambda=780$ nm and a pulse duration of 5 fs with an $\sin^2$ envelope. The FCP's peak intensity is around $I=10^{13}$ W/cm^2. For this testing calculation, we have used 256 partial waves in the expansion, with the largest total angular momentum $L=23$ and 8–12 combinations of $l_1 l_2$ for each L. We compare the calculated observables in Figs. 2(b) and 2(c), for cases of with and without potential-matrix optimization (discussed in Sec. III). Figures 2(b) and 2(c) show, respectively, the populations on the ground-state and on the *ps* partial wave ($l_1=1$, $l_2=0$) as a function of the interaction time. The black dashed line represents the case of optimization, while the red solid line stands for the case of without optimization (i.e., using the full matrix). We see that these curves are essentially identical, which means the optimization of decomposing the full matrix into small-matrices operations does not cause significant errors. We knew that for the block-diagonal electron-electron Coulomb potential the decomposition is exact, but for the block-tridiagonal laser-electron coupling matrix the alternative splitting can cause some errors, since the odd and even 2×2 blocks do not commute with each other. However, since we have arranged the odd and even block operations in a sandwich form [Eq. (21)], the noncommute errors are significantly reduced.

Next, we tested the speeding up of the FEDVR-TDCC code with the potential-matrix optimization for different number of total partial waves. The timing tests have been conducted on the Kraken (Cray XT5) supercomputer at the National Institute for Computational Sciences (NICS), by using 256 cores for the same problem discussed in Fig. 1. Results are shown in Figs. 3 and 4. In Fig. 3(a) we have compared the total time costs per step as a function of the

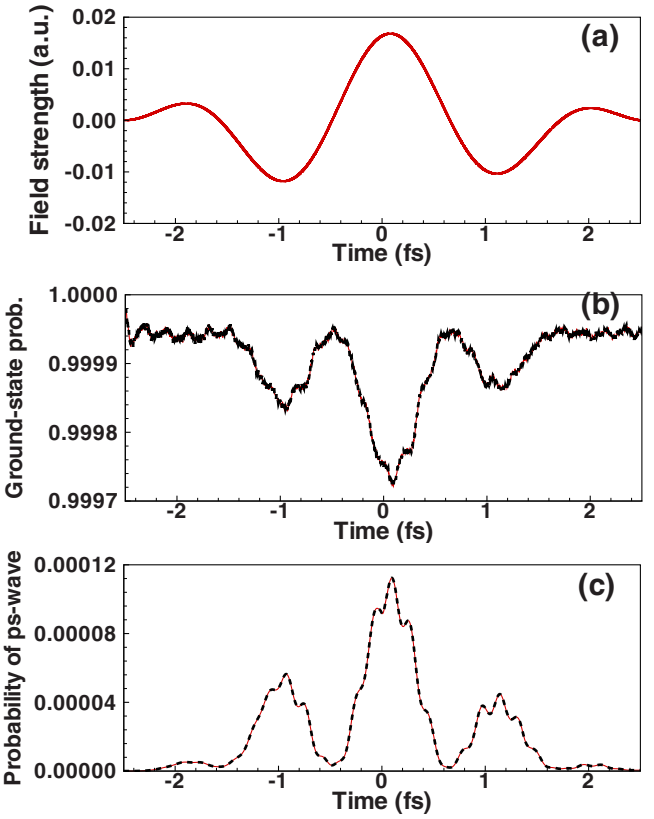

FIG. 2. (Color online) (a) A few-cycle laser pulse shape; (b) the ground-state population as a function of time in the cases of with (black dashed line) and without (read solid line) optimization; (c) same as (b) but for the probability of *ps*-partial wave.

total number (N) of partial waves used, for cases with and without optimization. The similar comparison of time cost for the total potential operations was plotted in Fig. 3(b). We see that at $N=32$ there is no much difference between the full potential-matrix operation (no optimization) and the optimized case. However, when the number of partial waves N increases the advantage of optimization shows up. At N

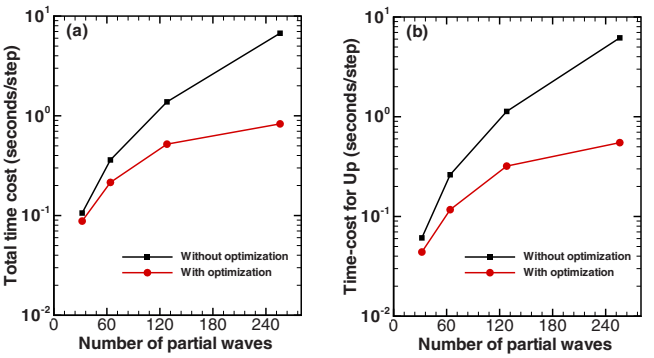

FIG. 3. (Color online) The comparison on time cost per step as a function of the number of partial waves used for TDCC expansion: (a) the total time cost and (b) the time cost only for the potential operation. Tests are performed with 256 cores on the NICS' Kraken (Cray XT5) supercomputer.

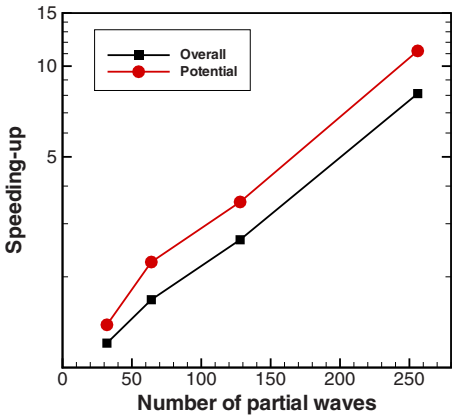

FIG. 4. (Color online) The overall speeding up of the FEDVR-TDCC code after optimization vs the total number of partial waves used in expansion. Tests are performed with 256 cores on the NICS' Kraken (Cray XT5) supercomputer.

$=256$, we get more than a factor of 10 faster for the optimized potential-matrix operation than that of without optimization.

Taking the time-cost ratio between no-optimization and optimization cases, we obtained a speeding up factor (f_{speeding}) that was plotted vs N in Fig. 4. We see that at $N=256$ the optimized potential operation got speeding up by more than an order of magnitude ($f_{\text{speeding}} \simeq 11.2$). If one uses the same number (n) of $l_1 l_2$ combinations to expand each L, then the total N partial waves are grouped into N/n blocks. Each block is a $n \times n$ nonzero matrix. In the full-matrix operations, we have separated the electron-electron Coulomb potential matrix and the laser-electron coupling matrix, since the latter has time dependence in the laser field. Thus, the full-matrix operations actually scale as $\sim O(2N^2)$ in our previous implementation. Now, the optimized electron-electron Coulomb potential takes only $\frac{N}{n} \times (n \times n) = nN$ operations, while the laser-electron coupling operations scale as $\sim \frac{3}{2} \times \frac{N}{2n} \times (2n \times 2n) = 3nN$. The factor of $\frac{3}{2}$ comes from the sandwich format, and 2×2-block matrix operation requires $2n \times 2n$ multiplications. In the end, we can estimate the speeding up factor to be $f_{\text{speeding}} = 2N^2/(nN+3nN) = N/2n \simeq 11.6$ for $N=256$ and $n \simeq 11$, which is consistent with our numerical testing results $f_{\text{speeding}} \sim 11.2$ (even though we have used a varied number of $n=8-12$.) Finally, the overall (including kinetic-energy operations) speeding up is about ~ 8.1. As the potential-energy operations weigh more in one time-step operation with increasing N, we expect more dramatical speeding up for $N > 256$.

V. SUMMARY

In summary, we have shown that the potential-energy matrix in the FEDVR-TDCC code can be further decomposed into a series of small matrices, due to its *block diagonal* and *block tridiagonal* structures of the electron-electron Coulomb potential and the linearly polarized laser-electron coupling. Specifically, the *block tridiagonal* electron-electron coupling is split into N/n operations of small $n \times n$ matrices, while the laser-electron coupling matrix is decomposed into even and odd $2n \times 2n$ matrices. Such optimization speeds up the total potential operation by a factor of $N/2n$, if each total angular-momentum L is expanded with the same number (n) of partial-wave combinations ($l_1 l_2$). Our numerical tests indicated more than ten times faster with such optimization at $N=256$. More dramatic speeding up is expected for large number of N partial waves. This may facilitate the long-sought solution to the 3D two-electron quantum dynamics in ultrashort intense optical laser pulses, and it may also find a variety of important applications such as electron-Rydberg-atom collisions. The technique we have proposed and demonstrated in this paper is particularly useful for the quantum-dynamics calculation of two-electron systems exposed to intense laser pulses. However, the similar idea of decomposing large matrix with many zeros to a series of small-matrix operations can be applied to other problems, for which one needs to work out the decomposing strategy specific to problems at hand.

ACKNOWLEDGMENTS

The author gratefully acknowledges the support by Laboratory for Laser Energetics at the University of Rochester and by the National Science Foundation (NSF) under the NSF-TeraGrid Grants No. PHY090093 and No. PHY100003. This work was conducted utilizing the NICS' Kraken Supercomputer.

[1] G. Tanner, K. Richter, and J. M. Rost, Rev. Mod. Phys. **72**, 497 (2000).
[2] D. N. Fittinghoff, P. R. Bolton, B. Chang, and K. C. Kulander, Phys. Rev. Lett. **69**, 2642 (1992).
[3] B. Walker, B. Sheehy, L. F. DiMauro, P. Agostini, K. J. Schafer, and K. C. Kulander, Phys. Rev. Lett. **73**, 1227 (1994).
[4] Th. Weber, M. Weckenbrock, A. Staudte, L. Spielberger, O. Jagutzki, V. Mergel, F. Afaneh, G. Urbasch, M. Vollmer, H. Giessen, and R. Dörner, Phys. Rev. Lett. **84**, 443 (2000).
[5] D. Dundas, K. T. Taylor, J. S. Parker, and E. S. Smyth, J. Phys. B **32**, L231 (1999).
[6] A. Becker and F. H. M. Faisal, Phys. Rev. Lett. **89**, 193003 (2002).
[7] X. Wang and J. H. Eberly, Phys. Rev. Lett. **103**, 103007 (2009); F. Mauger, C. Chandre, and T. Uzer, *ibid.* **104**, 043005 (2010).
[8] W. Becker and H. Rottke, Contemp. Phys. **49**, 199 (2008).
[9] M. S. Pindzola and F. Robicheaux, J. Phys. B **31**, L823 (1998).
[10] A. S. Kheifets and I. Bray, Phys. Rev. A **58**, 4501 (1998); J. Phys. B **36**, L211 (2003); I. A. Ivanov and A. S. Kheifets, *ibid.* **41**, 095002 (2008).

[11] A. Y. Istomin, N. L. Manakov, and A. F. Starace, J. Phys. B **35**, L543 (2002).
[12] B. Piraux, J. Bauer, S. Laulan, and H. Bachau, Eur. Phys. J. D **26**, 7 (2003); P. Antoine, E. Foumouo, B. Piraux, T. Shimizu, H. Hasegawa, Y. Nabekawa, and K. Midorikawa, Phys. Rev. A **78**, 023415 (2008).
[13] L. Feng and H. W. van der Hart, J. Phys. B **36**, L1 (2003).
[14] S. X. Hu, J. Colgan, and L. A. Collins, J. Phys. B **38**, L35 (2005).
[15] R. Shakeshaft, Phys. Rev. A **76**, 063405 (2007).
[16] D. A. Horner, C. W. McCurdy, and T. N. Rescigno, Phys. Rev. A **78**, 043416 (2008).
[17] X. X. Guan, K. Bartschat, and B. I. Schneider, Phys. Rev. A **77**, 043421 (2008); X. Guan, O. Zatsarinny, K. Bartschat, B. I. Schneider, J. Feist, and C. J. Noble, *ibid.* **76**, 053411 (2007); J. Feist, S. Nagele, R. Pazourek, E. Persson, B. I. Schneider, L. A. Collins, and J. Burgdörfer, *ibid.* **77**, 043420 (2008).
[18] J. S. Parker, L. R. Moore, K. J. Meharg, D. Dundas, and K. T. Taylor, J. Phys. B **34**, L69 (2001).
[19] J. S. Parker, B. J. S. Doherty, K. T. Taylor, K. D. Schultz, C. I. Blaga, and L. F. DiMauro, Phys. Rev. Lett. **96**, 133001 (2006).
[20] M. Witthoeft, J. Colgan, M. S. Pindzola, C. P. Ballance, and D. C. Griffin, Phys. Rev. A **68**, 022711 (2003).
[21] T. N. Rescigno and C. W. McCurdy, Phys. Rev. A **62**, 032706 (2000).
[22] B. I. Schneider and D. L. Feder, Phys. Rev. A **59**, 2232 (1999).
[23] B. I. Schneider and N. Nygaard, J. Phys. Chem. A **106**, 10773 (2002).
[24] B. I. Schneider, L. A. Collins, and S. X. Hu, Phys. Rev. E **73**, 036708 (2006).
[25] R. F. Lu, P. Y. Zhang, and K. L. Han, Phys. Rev. E **77**, 066701 (2008).
[26] L. A. Collins, J. D. Kress, and R. B. Walker, Comput. Phys. Commun. **114**, 15 (1998); B. I. Schneider and L. A. Collins, J. Non-Cryst. Solids **351**, 1551 (2005).
[27] M. S. Pindzola and F. Robicheaux, Phys. Rev. A **54**, 2142 (1996); M. S. Pindzola and F. J. Robicheaux, *ibid.* **57**, 318 (1998); M. S. Pindzola, *et al.*, J. Phys. B **40**, R39 (2007).
[28] S. X. Hu and L. A. Collins, Phys. Rev. A **71**, 062707 (2005).
[29] S. X. Hu and L. A. Collins, Phys. Rev. Lett. **96**, 073004 (2006).
[30] S. X. Hu and L. A. Collins, J. Mod. Opt. **54**, 943 (2007).
[31] S. X. Hu, Phys. Rev. A **74**, 062716 (2006).
[32] S. X. Hu, Phys. Rev. Lett. **98**, 133201 (2007).
[33] D. A. Horner, J. Colgan, F. Martin, C. W. McCurdy, M. S. Pindzola, and T. N. Rescigno, Phys. Rev. A **70**, 064701 (2004).
[34] J. Colgan, M. S. Pindzola, and F. Robicheaux, J. Phys. B **37**, L377 (2004).